



Radiation and Chemical Reaction Effects on Unsteady Magnetohydrodynamics Boundary Layer Fluid Flow in Porous Media

S.A.Amo, A.K.Adamu and O. Henry

Department of Mathematics and Statistics, Federal University Wukari, P.M.B. 1020, Wukari, Nigeria

ARTICLE INFORMATION

Article history:

Received 3 March 2019

Revised 8 March 2019

Accepted 15 March 2019

Available online 25 March 2019

Keywords:

Thermal radiation, Chemical reaction, unsteady MHD fluid flow

ABSTRACT

This study was conducted to investigate radiation and chemical reaction effects on unsteady MHD boundary layer flow in porous media over an exponentially stretching surface. In the study, boundary layer flow, heat and mass transfer of incompressible viscous unsteady MHD fluid over porous stretching vertical surface in the presence of thermal radiation was investigated. A similarity transformation was used to reduce the governing system of partial differential equations (PDEs) to a set of nonlinear Ordinary Differential Equations (ODEs) which were solved numerically using computer embedded fourth-order Runge-Kutta method with shooting technique. The results showed that an increase in radiation produced a rise on the velocity, temperature and concentration profiles. Skin friction, Nusselt and Sherwood numbers increased with increasing radiation.

1. Introduction

In boundary layer phenomena, radiation and chemical effects on unsteady MHD fluid flow, heat and mass transfers in porous media is significant because of its influence exponentially stretching porous surface. The unsteady MHD fluid flow study keeps paving ways for further studies due to its enormous usage in every facets of life. The investigation such as this can be modeled and solved experimentally, analytically or numerically depending on the nature of the modeled equations. In doing this, the existing models are modified or adjusted to reflect the current trends that are germane to the issues being discussed. In this presentation, efforts are made to reflect the effects of some unsteady MHD parameters in explaining pollutions in porous media. MHD fluid flow in porous media has wide and numerous applications in industry and environments [1]. Some of other areas of applications of this study though not limited are the flow of ground water through soil and rocks (porous media) that are very important for agriculture and pollution control; extraction of oil and natural gas from rocks which are prominent in oil and gas industries; functioning of tissues in body (bone, cartilage and muscle and so on) belong to porous media, flow of blood and treatments through them; understanding various medical conditions (such as tumor growth, a formation of porous media) and their treatment (such as injection, a flow through porous media in medical sciences).

In [1], viscous dissipative heat was taken into account under the influence of transverse magnetic field, [2] reported the heat and mass transfer in the boundary layers on an exponentially stretching continuous surface. Also, [3] presented the effects of heat generation and thermal radiation on steady MHD flow near a stagnation point on a stretching sheet in porous medium and presence of variable thermal conductivity and mass transfer, it was discovered that temperature increased with increasing radiation parameter R and concentration decreased with increasing Schmidt number.

Unsteady MHD flow and heat transfer of Nanofluid over a permeable shrinking sheet with thermal radiation and chemical reaction was analysed [4]. The analysis of unsteady free convective flow and mass transfer through a viscous, incompressible electrically conducting fluid along a porous vertical isothermal non-conducting uniformly decaying heat generation and transverse magnetic field with variable suction and viscous dissipation was performed [5]. Unsteady MHD flow of a viscoelastic fluid along vertical porous surface with fluctuating temperature and concentration was presented [6]. [7] verified the unsteady MHD flow and heat transfer for Newtonian fluids over an exponentially stretching sheet. [8] presented thermal radiation effects on heat and mass transfer of MHD flow in porous media over exponentially-stretching surface but neglected unsteady case. In 2018, an adaptive MHD convective fluid in porous media was presented [9]. The authors critically discussed the applications of the adaptive model to environmental issues. In view of the above studies, the present study examined the radiation and chemical effects on heat and mass transfer of unsteady MHD in porous media over an exponentially stretching porous surface. Specifically, the paper contended that controls of environmental pollution, air and water should be our concern.

2. Materials and Method

Consider the free convective thermal radiation effect on heat and mass transfer of two dimensional unsteady MHD flow of an electrically conducting, unsteady, viscous and incompressible fluid past an exponentially stretching sheet under the action of thermal and solutal buoyancy forces. A uniform transverse variable magnetic field $B(x)$ is applied perpendicular to the direction of flow with chemical reaction is taking place in the fluid flow. The flow is assumed to be in the x -direction with y -axis normal to it. The plate is maintained at the temperature and species concentration T_w, C_w and free stream temperature and species concentration T_∞, C_∞ respectively. The physical model and equations governing the radiation and chemical effects on heat and mass transfer of two-dimensional but unsteady MHD fluid flow in porous media are:

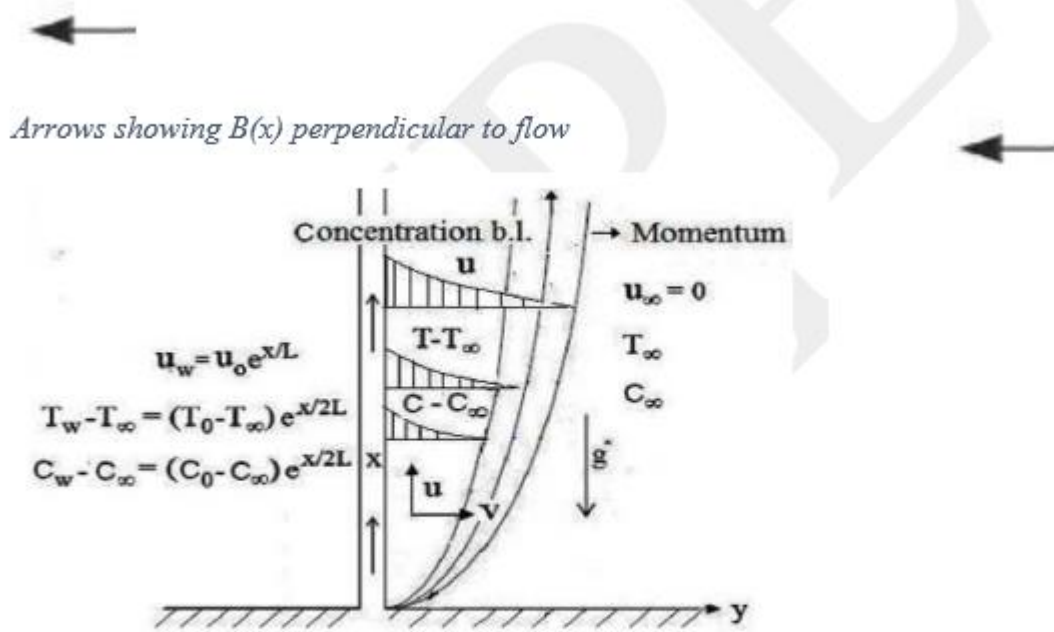


Figure 1 Showing the Physical Model and coordinate System

$$\frac{\partial u}{\partial x} + \frac{\partial v}{\partial y} = 0 \quad (1)$$

$$\frac{\partial u}{\partial t} + u \frac{\partial u}{\partial x} + v \frac{\partial u}{\partial y} = -\left(\frac{1}{\rho} \sigma B(x) + \frac{v}{K}\right)u + v \frac{\partial^2 u}{\partial y^2} + g\beta_T(T - T_\infty) + g\beta_C(C - C_\infty) \quad (2)$$

$$\rho C_p \left(\frac{\partial T}{\partial t} + u \frac{\partial T}{\partial x} + v \frac{\partial T}{\partial y} \right) = k \frac{\partial^2 T}{\partial y^2} - \frac{\partial q_r}{\partial y} + Q_0(T - T_\infty) \quad (3)$$

$$\frac{\partial C}{\partial t} + u \frac{\partial C}{\partial x} + v \frac{\partial C}{\partial y} = D \frac{\partial^2 C}{\partial y^2} - \gamma(C - C_\infty) \quad (4)$$

Subject to the following boundary conditions: (5)

$$u = U_0 \ell^{\frac{x}{L}}, v = -V_0 \ell^{\frac{x}{L}}, T = T_w = T_\infty + T_0 \ell^{\frac{x}{2L}}, C = C_w = C_\infty + C_0 \ell^{\frac{x}{2L}} \text{ at } y = 0$$

$$u \rightarrow 0, T \rightarrow T_\infty, C \rightarrow C_\infty \text{ as } y \rightarrow \infty, \frac{\partial u}{\partial t} \neq 0, \frac{\partial T}{\partial t} \neq 0, \frac{\partial C}{\partial t} \neq 0$$

where u , v , C , and T are velocity component in the x direction, velocity component in the y direction, concentration of the fluid species and fluid temperature respectively. L is the reference length $B(x)$ is the magnetic field strength, U_0 is the reference velocity, V_0 is the permeability of the porous surface respectively. The physical quantities K , ρ , v , σ , D , k , C_p , Q_0 and γ are the permeability of the porous medium density, fluid kinematics, viscosity, electric conductivity of the fluid, coefficient of mass diffusivity, thermal conductivity of the fluid, specific heat, rate of specific internal heat generation or absorption and reaction rate coefficient respectively while g is the gravitational acceleration, β_T and β_C are the thermal and mass expansion coefficients respectively. The q_r is the radiative heat flux in the y direction. By using the Rosseland approximation [3], the radiative heat flux q_r is given by

$$q_r = -\frac{4\sigma_0}{3\delta} \frac{\partial T^4}{\partial y} \quad (6)$$

Where σ_0 and δ are the Stefan-Boltzmann and the mean absorption coefficient respectively. We assume the temperature differences within the flow are sufficiently small such that T^4 may be expressed as a linear function of temperature, using Taylor series to expand T^4 about the free stream T_∞ and neglecting higher order terms, this gives the approximation

$$T^4 \cong 4T_\infty^3 T - 3T_\infty^4 \quad (7)$$

The magnetic field $B(x)$ is assumed to be in the form $B(x) = B_0 \ell^{\frac{x}{2L}}$ where the constant magnetic field is B_0 . Introducing the stream function $\psi(x, y)$ such that

$$u = \frac{\partial \psi}{\partial y}, v = -\frac{\partial \psi}{\partial x}, \quad (8)$$

Substituting (8) in (1), continuity equation satisfies Cauchy-Riemann equations and equations (2)-(4), gives

$$\frac{\partial \psi}{\partial t} + \frac{\partial \psi}{\partial y} \frac{\partial^2 \psi}{\partial x \partial y} - \frac{\partial \psi}{\partial x} \frac{\partial^2 \psi}{\partial y^2} = -\frac{\sigma}{\rho} B_0 \ell^{\frac{x}{2L}} \left(\frac{\partial \psi}{\partial y} \right) - \frac{v}{K} \left(\frac{\partial \psi}{\partial y} \right) + v \frac{\partial^3 \psi}{\partial y^3} + g\beta_T(T - T_\infty) + g\beta_C(C - C_\infty) \quad (9)$$

$$\frac{\partial \psi}{\partial t} + \frac{\partial \psi}{\partial y} \frac{\partial T}{\partial x} - \frac{\partial \psi}{\partial x} \frac{\partial T}{\partial y} = \left(\frac{k}{\rho C_p} + \frac{16\sigma_0 T_\infty^3}{3\rho C_p \delta} \right) \frac{\partial^2 T}{\partial y^2} + \frac{Q_0}{\rho C_p} (T - T_\infty) \quad (10)$$

$$\frac{\partial \psi}{\partial t} + \frac{\partial \psi}{\partial y} \frac{\partial^2 \psi}{\partial x \partial y} - \frac{\partial \psi}{\partial x} \frac{\partial^2 \psi}{\partial y^2} = -\frac{\sigma}{\rho} B_0 \ell^{\frac{x}{2L}} \left(\frac{\partial \psi}{\partial y} \right) - \frac{\nu}{K} \left(\frac{\partial \psi}{\partial y} \right) + \nu \frac{\partial^3 \psi}{\partial y^3} + g\beta_T (T - T_\infty) + g\beta_C (C - C_\infty)$$

$$\frac{\partial \psi}{\partial t} + \frac{\partial \psi}{\partial y} \frac{\partial T}{\partial x} - \frac{\partial \psi}{\partial x} \frac{\partial T}{\partial y} = \left(\frac{k}{\rho C_p} + \frac{16\sigma_0 T_\infty^3}{3\rho C_p \delta} \right) \frac{\partial^2 T}{\partial y^2} + \frac{Q_0}{\rho C_p} (T - T_\infty) \quad (11)$$

$$\frac{\partial C}{\partial t} + \frac{\partial \psi}{\partial y} \frac{\partial Q}{\partial x} - \frac{\partial \psi}{\partial x} \frac{\partial Q}{\partial y} = D \frac{\partial^2 C}{\partial y^2} - \gamma (C - C_\infty) \quad (12)$$

The corresponding boundary conditions become: (12)

$$\frac{\partial \psi}{\partial y} = U_0 \ell^{\frac{x}{L}}, \frac{\partial \psi}{\partial x} = V_0 \ell^{\frac{x}{L}}, T = T_w = T_\infty + T_0 \ell^{\frac{x}{2L}}, C = C_w = C_\infty + C_0 \ell^{\frac{x}{2L}} \text{ at } y = 0$$

$$\frac{\partial \psi}{\partial y} \rightarrow 0, T \rightarrow T_\infty, C \rightarrow C_\infty \text{ as } y \rightarrow 0$$

In order to transform the equations (9), (10) and (11) as well as the boundary conditions (12) into an ordinary differential equations, [10] introduced the following similarity transformations variables

$$\psi(x, y) = \sqrt{2\nu U_0 L} \ell^{\frac{x}{2L}} f(\eta), \eta = y \sqrt{\frac{U_0}{2\nu L}} \ell^{\frac{x}{2L}}, T = T_\infty + T_0 \ell^{\frac{x}{2L}} \theta(\eta), C = C_\infty + C_0 \ell^{\frac{x}{2L}} \phi(\eta) \quad (13)$$

The equations become (14)

$$f''' + ff'' - \frac{u}{2} - 2(f')^2 - (M + D_a)f' + G_r\theta + G_c\phi = 0$$

$$\left(1 + \frac{4}{3}R\right)\theta'' + P_r f\theta' - \frac{u}{2}P_r f'\theta + P_r Q_0\theta = 0 \quad (15)$$

$$\phi'' + S_c f\phi' - \frac{u}{2}S_c f'\phi - S_c \lambda\phi = 0 \quad (16)$$

The corresponding boundary conditions take the form: (17)

$$f = f_w, f' = 0.5, \theta = 0.5, \phi = 0.5, \text{ at } \eta = 0$$

$$f' = 0, \theta = 0, \phi = 0 \text{ as } \eta \rightarrow \infty$$

Where u is unsteady parameter, where M is the Hartman number, Gr is the thermal Grashof number, Gc is the solutal number, Q is the heat source, λ is the chemical reaction parameter, Sc is the Schmidt number, Pr is Prandtl number, Da is the Darcy porosity, R is the radiation parameter, f_w is the permeability at the plate. The equation (14), (15) and (16) are highly non-linear coupled differential equations and its satisfying the boundary conditions (17) are solved numerically by applying Nachtsheim-Swigert shooting iteration technique along with Runge-Kutta fourth-order integration scheme.

3. Results and Discussion

Numerical values of at the surface for different values of Pr. when newly introduced parameter was zero is presented in Table 1.

Table 1: Numerical Comparison of the present study at the surface for $\theta'(0)$

Pr.	M	R	$-\theta'(0)$ Present Study	$-\theta'(0)$ [8]
1			0.08333	0.09999
2			0.08333	0.10000
3			0.08333	0.10000
1	1	0	0.08333	0.09999
1	0	1	0.08333	0.09999
1	1	0	0.08333	0.09999

Therefore, the process of numerical computation for the skin friction coefficient, the Nusselt number and the Sherwood number which are respectively proportional to $f''(0)$, $\theta'(0)$, $\phi'(0)$, from this study at the plate have been examined for different values of the parameters are presented in Table 1 and discussed.

Table 2: Effect of $M, G_r, G_c, P_r, Q, \lambda, S_c, U, R, D_a,$ and f_w on $f''(0), \theta'(0)$ and $\phi'(0)$

P	VALUES	$F''(0)$	$-\theta'(0)$	$-\phi'(0)$
M	1	-0.3893	0.0728	0.2165
	2	-0.5647	0.0376	0.2096
	3	-0.7167	0.0089	0.2042
	4	-0.8515	0.0150	0.1998
Gr	1	-0.2900	0.0935	0.2207
	2	-0.0618	0.1536	0.2322
	3	0.1474	0.1927	0.2411
	4	0.3444	0.2220	0.2484
Gc	1	-0.2900	0.0935	0.2207
	2	-0.0781	0.1349	0.2296
	3	0.1273	0.1705	0.2376
	4	0.3271	0.2016	0.2457
Pr	0.71	-0.2900	0.0935	0.2207
	3	-0.3163	0.2927	0.2187
	3.5	-0.3214	0.3333	0.2182
	3.9	-0.3252	0.3647	0.2178
Q	-0.1	-0.3297	0.2582	0.2145
	0	-0.3198	0.2143	0.2160
	1	-0.3002	-0.0360	0.2075
	1.1	-0.2714	-0.1578	0.2108
λ	0.5	-0.2900	0.0935	0.2207
	1	-0.3006	0.0857	0.2828
	1.5	-0.3086	0.0804	0.3336
	2	-0.3152	0.0765	0.3774
Sc	0.24	-0.2900	0.0935	0.2207
	0.62	-0.3117	0.0808	0.3660
	0.78	-0.3182	0.0774	0.4154
	2.62	-0.3593	0.0610	0.8171

U	1	0.8293	0.1544	0.5941
	2	0.9060	0.0550	0.5392
	3	0.8911	0.0470	0.4792
	5	0.8578	0.0271	0.3924
R	0.5	0.8293	0.1544	0.5941
	1	0.6443	0.2283	0.8088
	1.5	0.3523	0.2850	1.0610
	2.5	0.0734	0.2777	1.3388
D_a	1	-0.2900	0.0935	0.2207
	3	-0.0224	0.2067	0.2207
	5	-0.9138	0.0254	0.1987
	7	1.1373	-0.0593	0.9197
f_w	0.1	-0.2900	0.0935	0.2207
	0.5	-0.3488	0.1166	0.2421
	1.0	-0.4523	0.1873	0.2705
	1.5	-0.6078	0.3408	0.3004

Table 2 represents the numerical results of variation in skin friction, Nusselt and Sherwood numbers at the surface with M , Da , f_w , Sc , Pr , R and λ which are of physical and engineering interest. It can be seen from the results that an increase in the values of M , Sc , Pr , Da , f_w , decrease the flow boundary layer while increase in values of Gr , Gc , Q , λ and R increase the flow boundary layer. Table 1 depicts that an increase in the values of M , Q , Sc , Da , R thicken the thermal boundary layer by reducing the rate at which heat diffuse out of the system while increase in Gr , Gc , Pr , f_w and Pr reduces the thickness of the thermal boundary layer. Also, the results showed that increase in Gr , Gc , Q , Sc , f_w , R causes thinning in the concentration boundary layer while M , Pr , Da thicken the mass boundary layer. The following graphs (Figures 2 -7) further elucidate the research work.

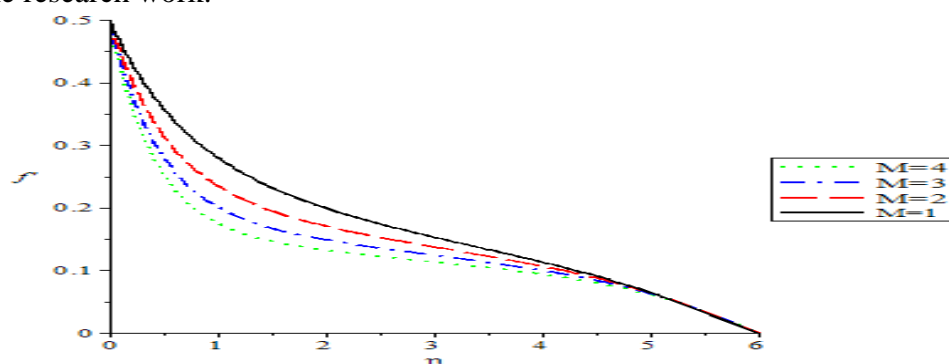


Figure 2: Velocity profile for the variation of Hartmann number M

Figure 2 shows that an increase in Hartmann's number led to decrease in velocity profile

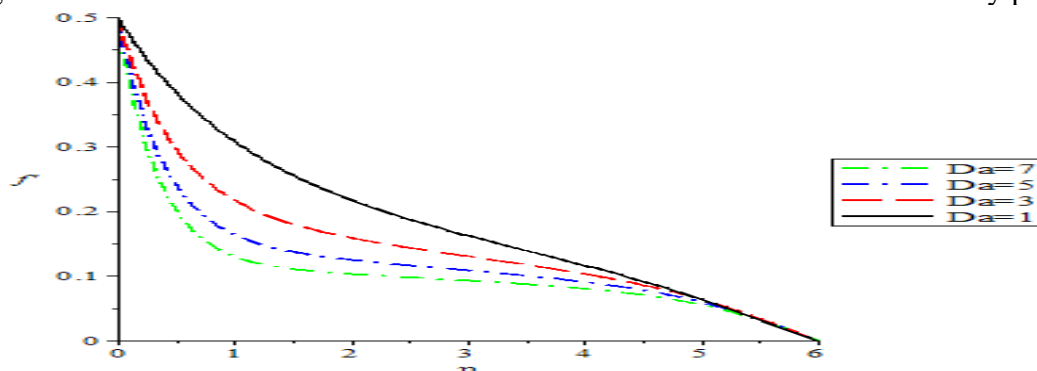


Figure 3: Velocity profile for the variation of Darcy Porosity Da

Figure 3 shows that an increase in Darcy porosity number led to decrease in velocity profile

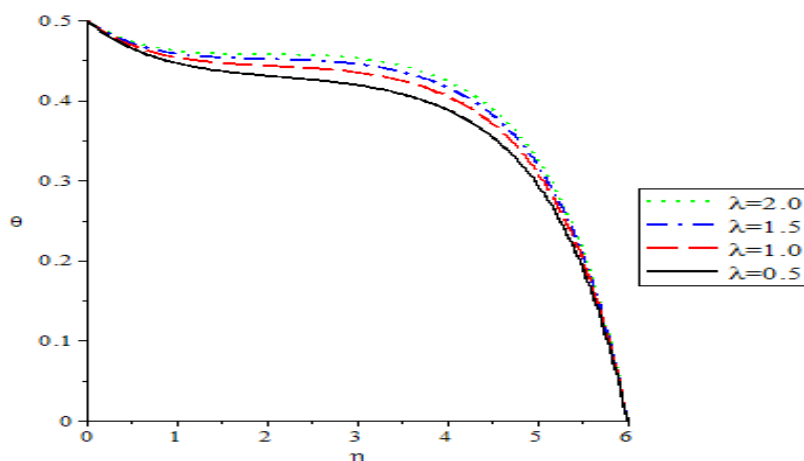


Figure 4: Temperature profile for the variation of the Chemical reaction λ

Figure 4 shows that an increase in chemical reaction λ led to increase in temperature profile. Its influence thereby increasing the rate at which the fluid was able to flow out of the system.

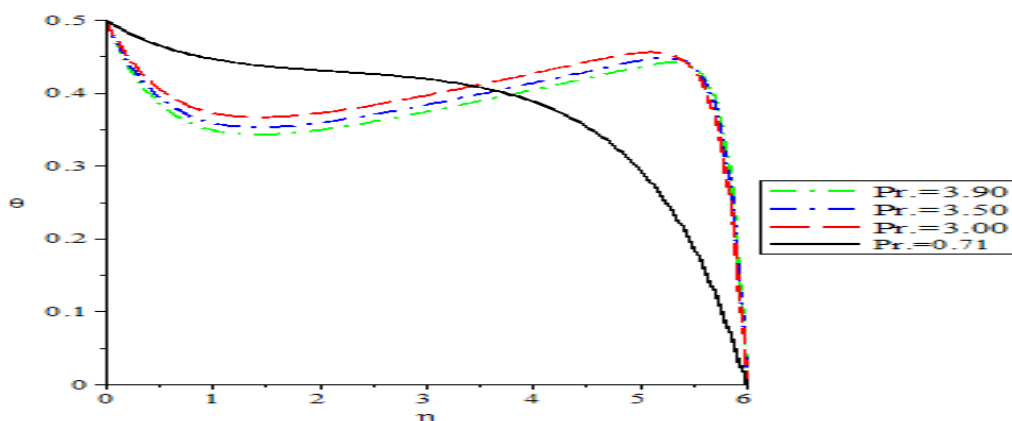


Figure 5: Temperature profile for the variation of the Prandtl number Pr.

Figure 5 shows that an increase in Prandtl number Pr. led to decrease in temperature profile. In this case Pr. decrease the thickness of thermal boundary layer and as a result, heat was able to diffuse out of the system thereby increasing the temperature profile.

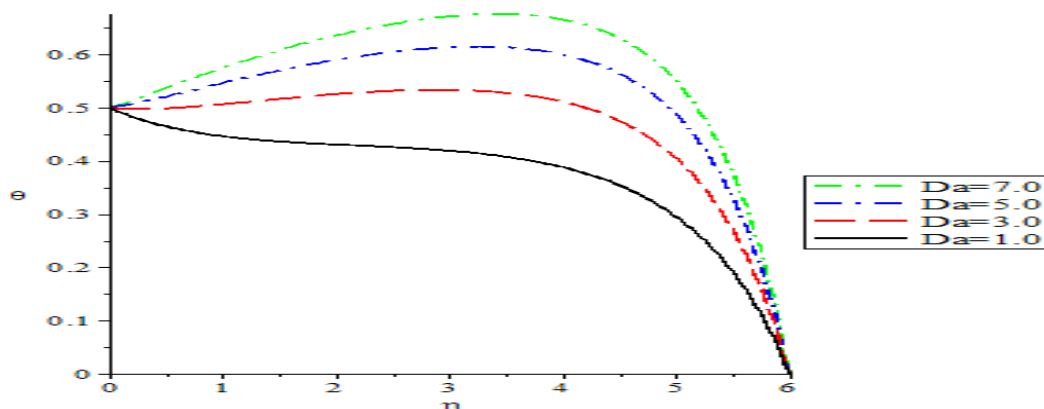


Figure 6: Temperature profile for the variation of the Darcy Porosity Da

Figure 6 shows that an increase in Darcy Porosity Da_c led to increase in temperature profile. Its effect on hydrological flow in sand soil did not permit turbulence hence porosity influences laminar flow.

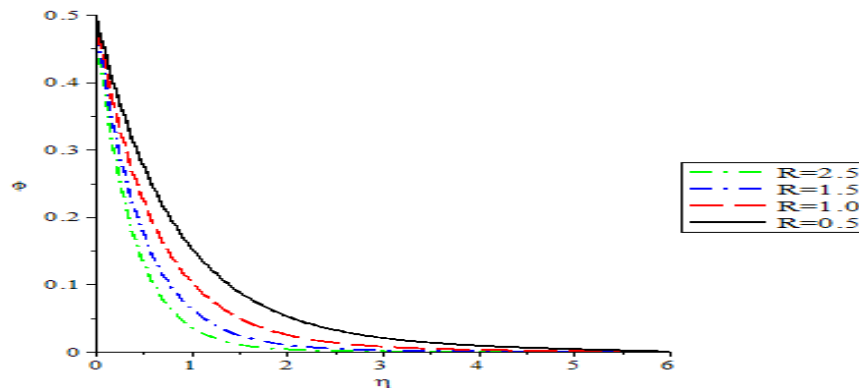


Figure 7: Concentration profile for the variation of the Radiation R

Figure 7 shows that an increase in Radiation R. led to decrease in concentration profile. Its decrease caused the thinning of mass boundary layer

4. Conclusion

In this study, a numerical analysis was presented to investigate the influence of radiation and chemical reaction effects on unsteady MHD boundary layer fluid flow in porous media. The non-linear and coupled governing equations were solved numerically by using fourth order Runge-Kutta scheme using Maple 18 software. Velocity, temperature and concentration profiles were presented graphically and explained appropriately. The fundamental independent parameters found to effect the problem under consideration were the Magnetic field parameter, Darcy porosity parameter, chemical reaction and Radiation parameter.

5. Acknowledgement

The authors wish to acknowledge all those whose papers were referenced.

6. Conflict of Interest

There is no conflict of interest associated with this work.

References

- [1] Kala, B. S., Singh, M. and Kumar, A. (2014) MHD free convection flow and heat transfer over non-linear stretching sheet embedded in an extended Darcy-forchhammer porous medium with viscous dissipation. *Journal of Global Research in Mathematics Achives*, 2(4), 1-14.
- [2] Magyari, E and Keller, B (1999), Heat and mass Transfer in the boundary layers on exponentially stretching continuous surface, *Journal of Physics, D: Apply Physics*. 32, 577-585.
- [3] Ibrahim, S. M. and Suneetha, K. (2015) Effects of heat generation and thermal radiation on steady MHD flow near a stagnation point on a stretching sheet in porous medium and presence of variable thermal conductivity and mass transfer. *Journal of Computational and Applied Research in Mechanical Engineering*. 4(2), 133-144.
- [4] Srivas, M. and Kishan, M. (2015) Unsteady MHD flow and heat transfer of Nanofluid over a permeable shrinking sheet with thermal radiation and chemical reaction. *American Journal of Engrn. Res*. 4(6), 68-79.

- [5] Sharma, P.R., Sharma, M. and Yadav, R.S. (2014). Viscous dissipation and mass transfer effects on unsteady MHD free convective flow along a moving vertical porous plate in the presence of internal heat generation and variable suction. *Int.J.Sci & Res. Publications: 4(9), 1-9*
- [6] Mohanty A., Rath, P.K. and Dash, G.C. (2014). Unsteady flow of a Visco-elastic fluid along the vertical porous surface with fluctuating temperature and concentration. *IOSR Journal of Engineering. 4(4) VI: 46 – 57.*
- [7] Hussain, S. and Ahmad, F. (2015) Unsteady MHD flow and heat transfer for Newtonian fluids over an exponentially stretching sheet. *Science International (Lahore), 27(2), 853-857.*
- [8] Amoo S.A. and Idowu A.S. (2017), Thermal radiation effects on heat and mass transfer of MHD flow in porous media over an exponentially stretching surface. In *FUW Trends in Science and Technology Journal e-ISSN 2408-5162, 2(1A), 33-41*
- [9] Amoo, S.A and Idowu, A. S. (2018) Adaptive MHD Convective Fluid in Porous media: panacea for Environmental controls. *Journal of the Nigerian Association of Mathematical Physics. 44 (January issue), 51-60.*
- [10] Sajid, M. and Hayat, T. (2008). Influence of thermal radiation on the boundary layer flow due to an exponentially stretching sheet. *International Communication Heat and Mass transfer, 35,347-356.*